FIFTH AUSTRALASIAN CONFERENCE

on

HYDRAULICS AND FLUID MECHANICS

at

University of Canterbury, Christchurch, New Zealand

1974 December 9 to December 13

EFFECT OF TRAILING EDGE THICKNESS ON THE AERODYNAMIC PERFORMANCE OF AEROFOILS

by

I. Lawrence & D. Lindley

SUMMARY

The flow around a two dimensional aerofoil with different trailing edge thicknesses was examined at Reynolds numbers between 6.9×10^5 and 1.1×10^6 (based on the aerofoil chord). Measurements were taken of the pressure distribution and the effect of the trailing edge thickness on these measurements is discussed. Traverses, using a hot wire anemometer, along and across the wake were taken to investigate the vortex formation point. These investigations showed that the vortex formation point varied between 0.75 and 1.2 times the trailing edge thickness downstream of the aerofoil.

A comparison was made between blunt trailing edges and a round trailing edge. The round trailing edge showed an increase in base pressure due to the separation point of the boundary layer 'rolling around' the trailing edge and thereby reducing the effective edge thickness.

Attempts were made to correlate the base pressure in terms of the aerofoil and boundary layer parameters, which although not successful did show the existence of a limiting value of the base pressure coefficient of approximately 0.25 for this particular aerofoil shape.

I. Lawrence, N.Z.E.D., Hamilton, N.Z.
D. Lindley, University of Canterbury, N.Z.

Introduction

Interest in the theoretical and experimental estimation of drag on bluff bodies has been with us at least since Kirkoff's solution to the pressure distribution around a circular body. From this approach there have been developed a number of solutions which can be classed as 'free stream line' theories.

Parallel to this there have been extensive experimental programmes (1), (2), (3) to investigate the pressure distribution and drag on bluff bodies, and the formation and decay of vortices in the wake. These experimental programmes have more recently, with the increasing interest in supersonic flight, been extended to isolated aerofoils with thick trailing edges in an effort to estimate the base pressure drag. These programmes, however, do not for the most part include the off design, or subsonic case, which has lead to a sparseness in experimental data. Interest in the base drag has extended to the turbine industry, so that more accurate estimations of the blade losses may be made. (4)

The base pressure behind a body is created by the separated boundary layers merging at a point downstream of the body, and so forming a separation cavity, from which fluid is entrained by the boundary layer, where the base pressure is defined by

$$C_{pb} = - \frac{P_b - P_\infty}{1/2 \rho U_\infty^2}$$

An experimental program was set up to investigate the variation of the pressure distribution and base pressure with trailing edge thickness and Reynolds numbers at low speeds.

Experimental Arrangement

The experiments were performed in a closed return wind tunnel having a working section of 920 mm x 1210 mm. The tunnel speed ranged from 0 to 42.5 m/sec giving Reynolds numbers up to 1.1×10^6. The turbulence level with the model in the tunnel varied from 0.5 percent to 1 percent at all speeds.

The model used was a truncated C4 aerofoil with a span of 660 mm and a chord of 470 mm. The aerofoil was truncated 21 percent and different trailing edge sections, four blunt and one round, attached. See table 1 for aerofoil semi co-ordinates.

A row of pressure tappings was inserted at the central span to measure the pressure distribution along the different trailing edge sections, by means of a multitube manometer bank, adjusted to the static pressure of the wind tunnel.

The flow in the wake was investigated by traversing a DISA constant temperature anemometer along and across the wake. The aerofoil surface boundary layers were measured in a similar manner.

The tunnel temperature and differential pressure were recorded so that the results could be corrected to standard atmospheric conditions.

Discussion of Experimental Results

The experimental work can be separated into three parts:

- Measurement of the pressure distribution,
- Wake investigation and
- Boundary layer profiles.

(i) Pressure Distribution.

It was assumed when measuring the pressure distribution, that the flow was essentially two dimensional.

Figure 1 shows the pressure distribution on the aerofoil with different trailing edge sections. A comparison of the various plots indicates that for $t/c = 0.033$ (round trailing edge) and $t/c = 0.039$, the increase in the pressure along the aerofoil are very similar except for the base pressure, which is lower for the blunt trailing edge. A further comparison between the round trailing edge and the other sections shows that for the pressure distribution for $t/c = 0.018$ and 0.027 there is an abrupt increase in the pressure at 8 percent chord upstream from the trailing edge. This increase in pressure is similar to that accuring in a boundary layer reattachment region, but closer examination showed that it could be attributed to the join in the aerofoil section, (join between the truncated section and trailing edge section). For the other trailing

edge section, t/c = 0.035, the pressure distribution is as predicted by thin aerofoil theory, except that C_p is lower at 100 percent chord than predicted by theory.

A 'full' comparison of the pressure distribution for t/c = 0.033, 0.035 and 0.039 shows that the trailing edge influences on the pressure distribution becomes negligible within approximately 80 percent of the chord, from the leading edge.

The differences in pressure distribution apparent in figure 1 are due to the slight changes in incidence of the aerofoil when the measurements were taken.

Measurements taken at 95 percent of the chord from the leading edge showed that vortices influenced the pressure distribution, as it was possible to record frequencies of approximately half the vortex shedding frequency. This effect was most evident on the round trailing edge section. The effect of the vortices can adequately be demonstrated with cylinders by measuring lift and drag as found by Rosko (2), (3).

From a plot of the base pressure coefficient versus Reynolds number in figure 2, it can be seen that as t/c increases the base pressure coefficient decreases, but is essentially independent of Reynolds number except for t/c = 0.035 and 0.039.

For t/c = 0.018 the base pressure coefficient is higher than predicted by Nash's theory (6), but a close examination of the semi-coordinates, table 1, showed that the trailing edge section was essentially boat tailed. The effect of this is to decrease the length of the separation cavity and to reduce the influence of the vortex.

The plot of C_{pb} versus t/c, figure 3, shows the trend, that as t/c increases, the base pressure decreases, approaching a minimum value of 0.25.

This trend can be explained as follows. When the boundary layers separate from the trailing edge they can be considered as free shear layers. These free shear layers are subject to a negative pressure gradient which tends to collapse them, so that they merge at a point downstream of the aerofoil to form a cavity.

The negative pressure gradient is dependent on the local conditions, so that the collapse of the free shear layers will be the same for similar stream conditions. Hence the further apart the boundary layer separation points, the greater will be the distance downstream that the free shear layers merge.

The collapse of the free shear layers is not entirely due to the negative pressure gradient but is assisted by the entrainment of fluid from the separation cavity, by the free shear layer. The fluid entrainment lowers the pressure inside the separation cavity.

The effect of the collapse of shear layer is to increase the local velocities of the stream lines, which influences the vortex formation and their influence on the base pressure.

(ii) Wake Investigation.

The wake was traversed using a hot wire anemometer to find the vortex formation point by measuring the maximum velocity fluctuations in the stream wise direction. A similar method has been used by a number of researchers (7), (8) who found that the point of maximum velocity fluctuation could be considered to be a good first approximation as the vortex formation point.

In figure 4 a plot of φ ($= \frac{U_{rms}}{U_\infty} \times 100$) versus distance downstream for the different trailing edge thicknesses, shows that as t/c decreases the velocity fluctuations decreases as the vortex strength decreases. This decrease in φ also indicates an increase in the vortex shedding frequency. This shedding frequency increase was subsequently measured. For each trailing edge section φ decreased slightly, less than 2 percent with increasing Reynolds numbers, but could be considered essentially constant.

Inside the separation cavity the fluid velocities varied between 12 and 20 percent of the free stream velocity for t/c = 0.018 and 0.039 respectively. The R.M.S. velocity decreased inside the separation cavity for decreasing trailing edge thickness, reflecting the decreasing strength and influence of the vortices, on the base pressure.

A plot of Strouhal number (based on trailing thickness) versus the Reynolds

number, figure 5, shows an increase in shedding frequency as t/c decreases, indicating, as above that the vortex strength is decreasing. This decrease in vortex strength will decrease the width of the wake close to the trailing edge at low speeds. The wake will, as a consequence, recover more quickly as t/c decreases. Measurements were taken to assess the wake recovery, and it was found that for t/c = 0.039, 0.033 and 0.035 the vortex shedding frequencies could be measured between 25 percent and 40 percent chord downstream of the aerofoil. The shedding frequency for t/c = 0.033 was the 'weakest' recorded, indicating a greater rate of wake recovery than for t/c = 0.039 and 0.035. For t/c = 0.027 and 0.018 the frequencies could not be measured at 25 percent chord downstream showing that the vortices had already been dissipated in the wake.

A comparison of these measurements would suggest that as t/c decreases the vortex strength is decreasing as the rate of wake recovery increases, as was found by Lieblein and Rondebush (11).

An examination of figures 2 and 5 suggests that:

$$S = f\ (C_{pb})^n$$

where f is a function of free stream velocity and the vortex velocity relative to the free stream velocity.

Attempts to derive a universal Strouhal number of the above form have been made by Rosko (9) and Bearman (10) but with no notable success. This is due to the number of unknowns, such as vortex spacing, width of the wake and the amount of available vorticity that goes into individual vortices. No calculations were made to estimate the required parameters in the experimental programme described here.

(iii) Boundary layer.

The boundary layer profiles, figure 6, were obtained using a hot wire anemometer by measuring the velocities at 95 percent chord from the leading edge where the pressure coefficient for the different trailing edge sections changed very little, (figure 1).

The general condition of the boundary layers was an intermediate profile, i.e. neither laminar nor turbulent, H varied between 1.5 and 1.9 and the turbulence level between 3 percent and 5 percent, based on the free stream velocity, increasing with Reynolds number, for all trailing edge sections.

A plot of the boundary layer profiles, figure 6, for different t/c shows that the profile is fuller as t/c increases and that the boundary layer thickness is decreasing at the same time. This increase in 'fullness' and decrease in thickness is caused by the decreasing aerofoil curvature, allowing the boundary layer to develop as on a flat plate. There is as a consequence of the above change a decrease in the skin friction as can be seen from figure 7, a plot of t/θ versus C_{pb}.

This correlation is compared with Hoerner's (12) but produces a scatter of 25 percent. It does however show the same trend, i.e. tending to minimum value of $C_{pb} = 0.25$ for $t/\theta = 13$.

A comparison with Hoerner's correlation and the experimental results indicates the influence of the vortices have on the base pressure. Hoerner's correlation is obtained using data from high speed experiments where the flow is essentially steady, and data where vortex was suppressed by means of a step. This is reflected by the fact that t/c = 0.018 falls below and t/c = 0.027 falls on Hoerners line. These two sections had highest rate of wake recovery and the weakest vortices. For t/c = 0.033 (round trailing edge) C_{pb} falls below the line as the vortex influence on the base pressure is reduced.

The high base pressure for t/c = 0.033, shown in figures 2, 3, and 7 is created by the boundary layer curving around the trailing edge, and effectively reducing the trailing edge thickness and the vortex strength. (See Nash et al (13)).

The rolling around of the separation point of the boundary layer was observed when the aerofoil was painted to test for boundary layer separation.

Concluding Remarks

In order to assess the effect of the base pressure drag as the trailing edge thickness increases, a criterion must be established for thinness. Nash (14) has correlated data which shows that for t/c between 0 and 0.002 the drag

can be accurately estimated using Squire and Young's theory. For $t/c > 0.002$ it is found that the base pressure drag must be included to obtain an accurate estimate, where the base pressure drag is defined as

$$C_{pb} (1/2\rho U_\infty^2)$$

The drag coefficient measured in the present experiments was obtained by traverses at 50 percent chord downstream, where the mixing losses would be present. The values obtained varied between 0.0018 for $t/c = 0.018$ and 0.02 for $t/c = 0.039$, there being little variation of the drag coefficient with Reynolds numbers for each trailing edge.

Calculations were made to check the thinness criteria using the boundary layer momentum thickness obtained from the experiments and using Squire and Young's theory. The differences obtained varied from 8 to 25 percent lower for $t/c = 0.018$ and $t/c = 0.039$ respectively, but with the inclusion of the base pressure drag and agreement was within 5 percent. The best agreement was for the round trailing edge and $t/c = 0.018$.

The drag coefficient was calculated using Nash's theory (6) and it exhibited the same differences as above but in this particular case it was due to the neglect of the vortex street in the wake analysis. These calculations effectively demonstrated the effect of the vortex on the base pressure.

From a comparison of the correlations in figure 7, it is apparent that 'no two' aerofoils are the same, as minor differences can effect the vortex street formation. This can be demonstrated by experiments using short and long splitter plates (7) (13). It is also evident from the literature that attempts to correlate the base pressure coefficient with Strouhal number are unsuccessful as the spacing; and energy of the vortex can be altered by minor structural differences.

The vortex formation point as a function of the trailing edge thickness does however show a general trend and appears to occur one trailing edge thickness downstream. This criterion would allow a solution to the pressure distribution around a thick trailing edge aerofoil by extending its length by one trailing edge thickness and assumming the trailing edge to be sharp. It would not however account for the increased vortex influence with trailing edge thickness, nor would it account for the differences between blunt and round trailing edges.

Notation.

t	trailing edge thickness
c	chord
$U\infty$	free stream velocity (upstream)
Urms	R.M.S. of velocity fluctuations
P_b	Base pressure
$P\infty$	free stream pressure
P	static pressure on aerofoil surface
C_{pb}	base pressure coefficient
C_p	pressure coefficient $(P - P\infty) / (1/2\rho U\infty^2)$
θ	momentum thickness
ρ	fluid density

References.

(1) Faye, A. and Johnson, F.G. (1927) A.R.C. R and M 1104 and A.R.C. R and M 1143
(2) Rosko, A. (1954) N.A.C.A. TN 3169
(3) Rosko, A. (1955) N.A.C.A. TN 2913
(4) Denton, J. (1971) C.E.G.B. Rep. RD/M/R148
(5) Bellhouse, B.J. and Wood, C.I. (1965) Jl. Roy Aero Soc.
(6) Nash, J.F. (1964) A.R.C. R and M 3436
(7) Bearman, P.W. (1965) Jl. Fluid Mech Vol 21
(8) Schaefer, J.W. and Eskinazi, S. (1959) Jl. Fluid Mech. Vol. 6
(9) Rosko, A. (1955) Jl. Aero Sc. Vol 22
(10) Bearman, P.W. (1967) Jl. Fluid Mech. Vol 28
(11) Lieblein, S. and Rondebush, W.H. (1956) N.A.C.A. TN 3771
(12) Hoerner, S.F. (1965) 'Fluid dynamic drag' Pub. by Anthor
(13) Nash, J.F. Quincey, G.G. and Callinan, J. (1963) A.R.C. R and M 3427
(14) Nash, J.F. (1965) N.P.L. Aero Rep. 1162.

TABLE 1

Nondimensional semicoordinates of truncated aerofoil and the trailing sections.

Truncated Section C4

Y/c	x/c
0.0	0.0
.020	.014
.033	.007
.044	.108
.050	.170
.053	.250
.053	.329
.050	.465
.045	.575
.043	.630
.039	.682
.035	.789

Trailing edge Sections

t/c = 0.018	t/c = 0.027	t/c = 0.033**	t/c = 0.035	t/c = 0.039
x/c	Y/c	Y/c	Y/c	Y/c	0.026
0.829	0.026	0.026	0.026	0.026	.023
.857	.021	.022	.023	.021	.021
.894	.015	.019	.019	.019	.020
.906	.010	.017	.017	.018	.020
.920	.009	.017	.017	.018	.020
.937	.009	.016	.017	.018	.019
.948	.009	.016	.017	.018	.019
.967	.009	.015	.017	.018	.019
.977	.009	.015	.017	.017	.019
1.000	.009	.014	.000	.017	.019

* Trailing sections t/c = 0.018, 0.027, 0.035, 0.039 are blunt trailing edge sections.

** t/c = 0.033 is a round trailing edge of radius 1.6 percent chord.

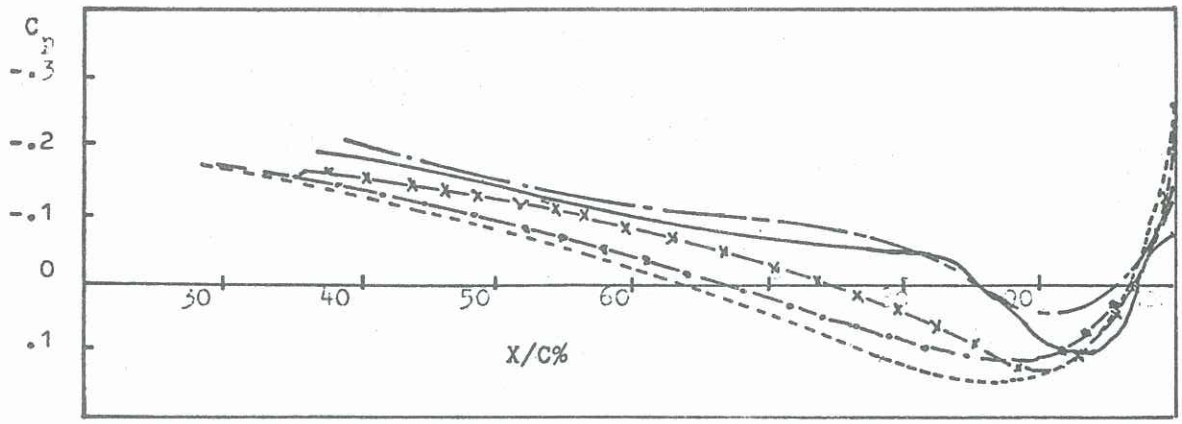

* FIGURE 1 Pressure distribution along aerofoil with different trailing edge sections.

*
NOTATION FOR FIGURES 1, 4 AND 6

———— t/c = .018
— – — t/c = .027
—·—·— t/c = .033
—X—X— t/c = .035
– – – – t/c = .039

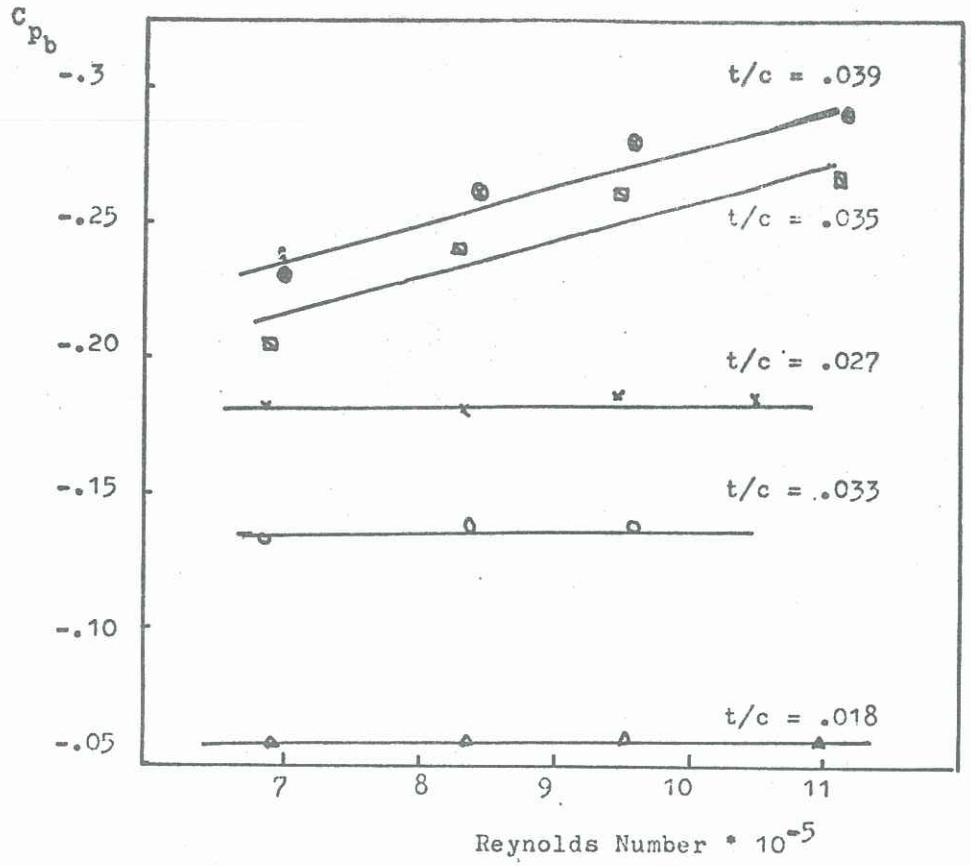

FIGURE 2 Base pressure coefficient versus Reynolds Number

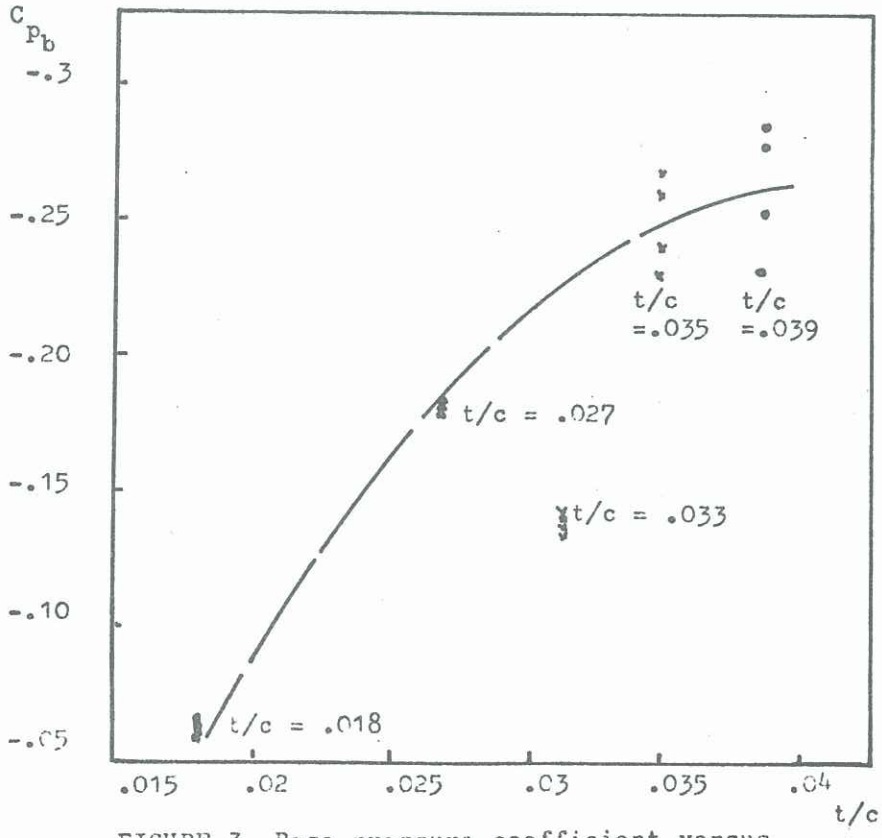

FIGURE 3 Base pressure coefficient versus (t/c)

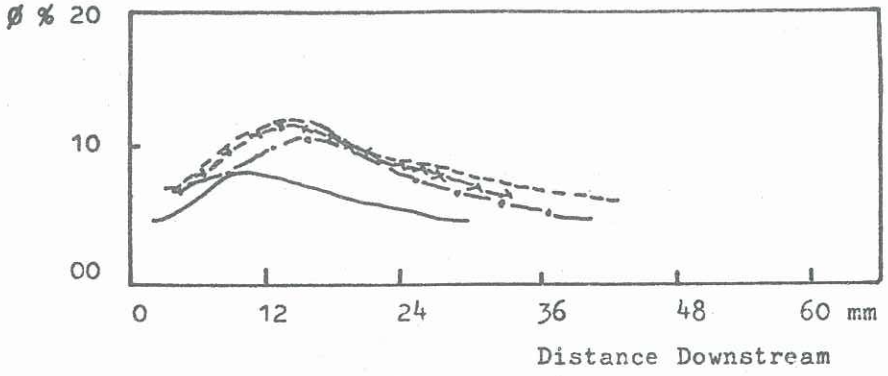

*FIGURE 4 Velocity fluctuation along the wake

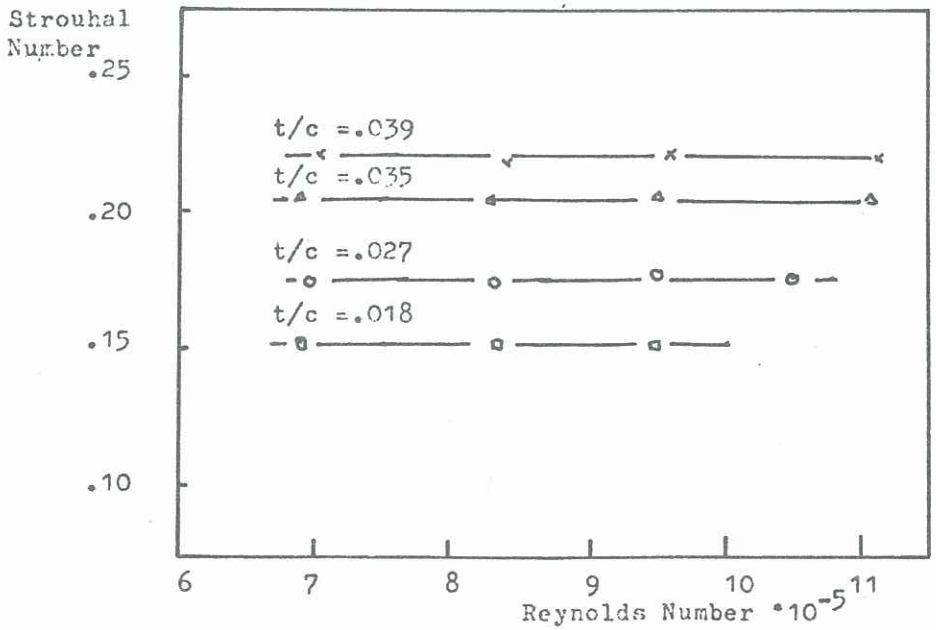

FIGURE 5 Strouhal Number versus Reynolds Number

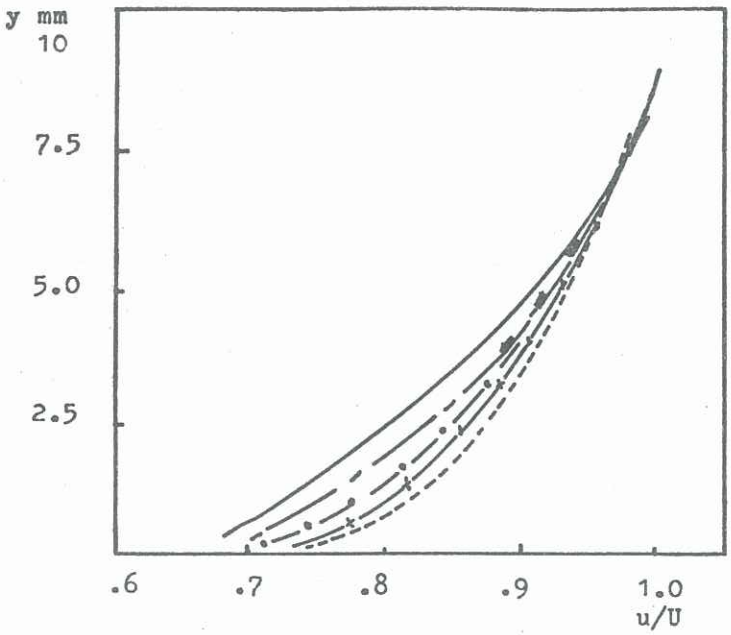

* FIGURE 6 Boundary layer profiles at the trailing edge ($Re = 9.5*10^5$)

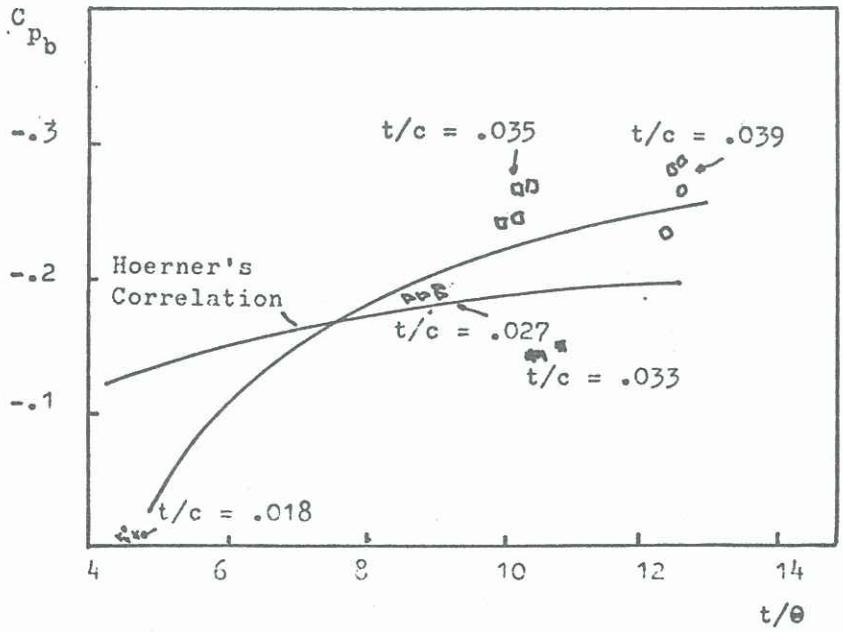

FIGURE 7 Base pressure coefficient versus (t/θ)